Plasma Sources Sci. Technol. **9** (2000) 517–527. Printed in the UK PII: S0963-0252(00)15592-6

Introduction to gas discharges

N St J Braithwaite

The Open University, Oxford Research Unit, Foxcombe Hall, Boars Hill, Oxford OX1 5HR, UK

Received 1 December 1999, in final form 13 June 2000

Abstract. This is a tutorial article. An introductory discussion of direct current gas discharges is presented. Beginning with basic ideas from kinetic theory, gas discharge plasmas are described in terms of phenomena observed in the laboratory. Various models are introduced to account for electrical breakdown, plasma boundaries and the longitudinal and transverse structure of discharges.

1. Introduction

This article is intended to set the scene for more detailed discussions about the physics of laboratory plasmas. There are many types of plasma source such as those based on discharges created by direct current (dc), capacitively coupled radiofrequency (rf) (RIE, PECVD), inductively coupled rf (ICP, TCP, Helicon) and microwaves (ECR, Surfatron). The technological applications of plasmas formed in these sources are numerous and include thin film deposition, semiconductor processing, materials treatments (modification of surface physics and surface chemistry, sterilization), lamps, light sources and displays, thick film deposition, waste treatment and materials analysis.

In section 2 some basic results from kinetic theory are recalled. The nature of the plasma state and of laboratory plasmas in particular is described in section 3. Sections 4 and 5 examine the production and loss of charged particles, including the breakdown phase of a gas discharge. In section 6 the spatial structure of a steady state, self-sustaining discharge is discussed, for medium and low pressure. A final brief section illustrates the flow of energy in a low-pressure, laboratory plasma.

2. Just particles

The kinetic description of a stationary gas considers large populations of gas atoms with a range (or distribution) of speeds moving in all directions. The distributions of speed and velocity are characterised by a mean energy, $\langle\varepsilon\rangle$, which is linked by the form of the distribution to the kinetic temperature, kT. Pressure, p, in a gas is a measure of the density of thermal energy associated with the number of gas atoms per unit volume, n_g. Thus,

$$p = n_g kT \tag{1}$$

(SI units: p is in Pa when n_g is in m^{-3} and kT is in J; one pascal is equivalent to a joule per cubic metre). Similar concepts apply to charged particle populations. In the following some more useful rabbits are pulled out of the hat of kinetic theory. Use will be made of the following data:

- radius of argon atom, $r_{Ar} = 1.5 \times 10^{-10}$ m;
- Boltzmann's constant, $k = 1.38 \times 10^{-23}$ J K^{-1};
- mass of argon atom, $M_{Ar} = 40 \times 1.67 \times 10^{-27}$ kg;
- mass of electron, $m = 9.11 \times 10^{-31}$ kg;
- electronic charge, 1.60×10^{-19} C.

2.1. Moving neutrals (in a thermalized group)

At room temperature the average speed of an argon atom (atomic mass 40) is 3.5×10^2 m s^{-1},

$$\bar{v} = \sqrt{\frac{2kT}{M}}. \tag{2}$$

At a pressure of 1 Torr (130 Pa) the random flux of argon atoms at room temperature is 2×10^{25} atoms m^{-2} s^{-1},

$$\Gamma = \frac{n\bar{c}}{4} = n\sqrt{\frac{kT}{2\pi M}}. \tag{3}$$

At a pressure of 1 Torr (130 Pa) the distance travelled by an argon atom between collisions will be on average about 0.11 mm,

$$\lambda = \frac{1}{4\sigma n_g} \tag{4}$$

$$\sigma = \pi r_{Ar}^2. \tag{5}$$

The frequency of collisions between gas atoms at room temperature is 3.5×10^6 s^{-1},

$$\nu = \frac{\bar{v}}{\lambda} \tag{6}$$

A flow of neutrals arises when there are gradients in pressure (i.e. gradients in density and/or temperature).

2.2. Moving charges

The introduction of charge changes a few things. First, charge is a source of electric field through which every charge exerts forces on any other charges in inverse square proportion to their separation (r^{-2}). Second, an externally imposed electric field will apply forces to any charges that enter it.

Third, charges that move relative to magnetic fields also experience forces. The Lorentz force conveniently combines the electric and magnetic effects for a charge

$$\boldsymbol{F} = q(\boldsymbol{E} + \boldsymbol{v} \times \boldsymbol{B}) \tag{7}$$

in which: q is the quantity of charge in coulombs; $\boldsymbol{E}$ is electric field in volts per metre; $\boldsymbol{v}$ is velocity in metres per second; $\times$ here implies the vector product; $\boldsymbol{B}$ is the flux density in teslas.

If work is done on a charge it gains energy

$$\tfrac{1}{2}mv_d^2 = eV \tag{8}$$

where v_d is a drift velocity. The energy eV can be gained by moving a given distance, x_1, in the direction of an electric field:

$$eV = \int_0^{x_1} eE \, \mathrm{d}x. \tag{9}$$

Elastic collisions randomize particle motions leading to a mean thermal speed as equation (2).

2.3. Elastic and inelastic collisions

By far the most common encounter in gases is between pairs of particles (binary collisions). When particles interact (collide) momentum and energy must be conserved. There are three clear classes of event.

(i) Elastic: momentum is redistributed between particles and the total kinetic energy remains unchanged, e.g.

$$\mathrm{e}^-_{fast} + \mathrm{A}_{slow} \rightarrow \mathrm{e}^-_{less\ fast} + \mathrm{A}_{less\ slow}.$$

(ii) Inelastic: momentum is redistributed between particles but a fraction of the initial kinetic energy is transferred to internal energy in one or more of the particles (i.e. excited states or ions are formed), e.g.

$$\begin{aligned}\mathrm{e}^-_{fast} + \mathrm{A} &\rightarrow \mathrm{e}^-_{slower} + \mathrm{A}^* \\ &\rightarrow \mathrm{e}^-_{slower} + \mathrm{A}^+ + \mathrm{e}^-.\end{aligned}$$

(iii) Superelastic: a third class also needs to be anticipated—here there is more kinetic energy after the collision. Momentum is conserved and internal energy in the particles entering into a collision is transferred into kinetic energy, e.g.

$$\mathrm{A}^*_{slow} + \mathrm{B}_{slow} \rightarrow \mathrm{A}_{faster} + \mathrm{B}_{faster}.$$

Detailed analysis of binary collisions reveals some useful general points.

- Lighter particles (m) cannot lose much energy elastically to heavier particles (M)—at best a fraction $2m/M$, nevertheless, substantial changes in momentum occur (cf tennis).
- A moving particle on striking elastically a stationary one of equal mass head-on can transfer all of its kinetic energy (cf billiards).
- Lighter particles can lose virtually all their kinetic energy through inelastic collisions with heavier objects (cf sandblasting).
- Equal mass particles can lose no more than half their kinetic energy inelastically on collision (cf ion impact ionization).
- Binary collisions in which at least one particle is charged may be dominated by long-range Coulomb forces.

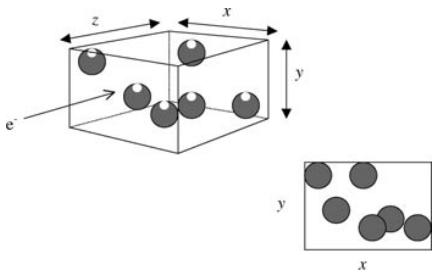

Figure 1. Calculation of mean free path.

2.4. Cross section and mean free path—elastic collisions

A thorough study of collisions considering scattering angles and impact parameters will be covered in a companion article. Here a simpler 'zeroth order' approach is presented to account for the more general features.

Consider an electron moving through a number of stationary argon atoms; see figure 1. Simple elastic encounters only will be dealt with here so the target atoms are viewed as hard spheres and the electron is assumed to behave as a point mass; effects arising from its charge are not included. The question to be addressed is how far the electron can be expected to penetrate before having a collision.

The number of target (argon) atoms in a cuboid xyz is $n_g xyz$. Each atom presents a cross section, $\pi r_{Ar}^2 = \sigma$, obscuring the electron path. Viewed through the face xy the total area blocked by atoms will be $n_g xyz\sigma$. When the cuboid extends as far as one mean free path (λ), virtually the entire face xy will be obscured so

$$(n_g xy\lambda)\sigma = xy \qquad \lambda = \frac{1}{n_g\sigma} \tag{10}$$

and the electron is very likely to have a collision (cf equation (4) which has a factor of four to account for the size of the projectile atom). From equation (6), the frequency of encounters can be *estimated* for projectiles, electrons in this case, with a mean speed $\bar{v}$

$$v = \bar{v} n_g \sigma. \tag{11}$$

The scaling of mean free path and frequency of collisions with pressure, through n_g, and energy, through $\bar{v}$, are consistent with intuition.

In practice cross sections are not actually independent of energy, even for elastic collisions. High-energy electrons speed past so quickly that the chances of interacting with the outer shell electrons on an atom are reduced. Also, at very low energy, quantum mechanics may prevail, taking an electron around an atom with a marked inability to interact over a narrow range of energy—the so-called Ramsauer effect. Figure 2 illustrates these features for argon, showing also inelastic cross sections. The simple hard sphere cross section is about 3×10^{-20} m^2.

3. Characterizing plasmas

3.1. Similarities and differences

All plasmas have a number of features in common. For instance, they are composed of equal amounts of positive

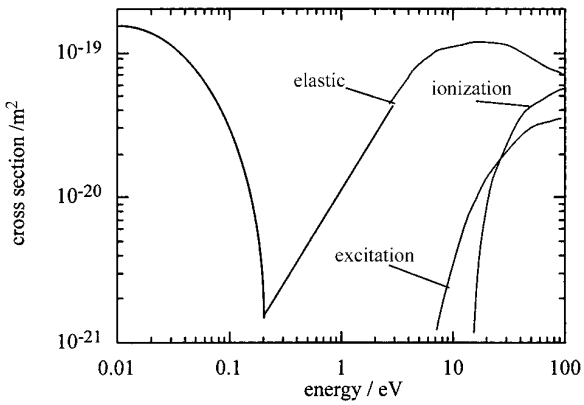

Figure 2. Cross sections for argon (approx./schematic).

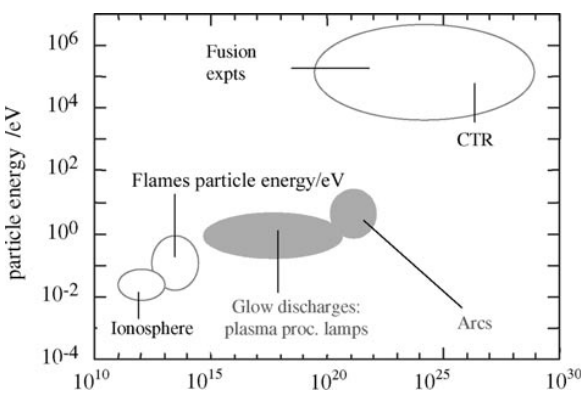

Figure 3. A 2D map of parameter space (density-energy).

and negative charge carried by particles that are arranged without any local ordering, being free to move. One way to begin a classification is to quantify: (i) the density of the charge carriers (so many per cubic metre); and (ii) the thermal energy of electrons in particular. Figure 3 shows this kind of two-dimensional (2D) classification of plasmas.

Even within a small region of the density–energy parameter space there are innumerable distinctly different plasmas. For example, a plasma containing electrons and argon ions is distinguishable from one containing negative ions and positive ions formed from fragments of a molecule of sulphur hexafluoride.

3.2. Equilibrium and steady states

The plasma state can be realised as a thermal equilibrium phase of matter beyond the conditions of gases. However, just as amorphous solids appear to be steady-state (though non-(thermal)-equilibrium) solids, so too laboratory-generated plasmas often exist as steady, non-(thermal)-equilibrium states. It must be noted also that the lifetime of individual particles in laboratory plasmas may only be a small fraction of a second, so the steady state is a kind of dynamic (but non-thermal) equilibrium.

3.3. Laboratory plasmas—sustaining the steady state

Early laboratory experiments in which capacitors were discharged through a gas provided transient sources of

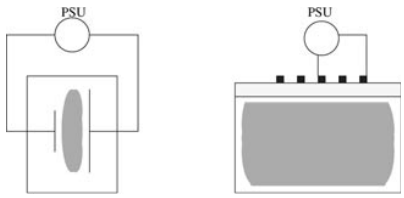

Figure 4. Confined (laboratory) plasmas.

ionized gas. Nowadays, continuous electrical discharges are often used to create a dynamic steady state in which there is a balance between production (sources) and loss (sinks). An overflowing water tank maintains a dynamic steady state as water flows out at the same rate as it flows in. If the production and loss processes are physically separated, as often is the case for laboratory plasmas that are non-(thermal-) equilibrium, then energy invested in production is effectively transported to the place of loss and a steady flow of energy must be supplied to sustain the steady state.

Laboratory plasmas are formed when gas is ionized by driving an electric current through it, or by shining electromagnetic radiation into it. Generally, these means of plasma formation give energy directly to the free electrons in the plasma. Electron–atom collisions then liberate more electrons and to some degree heat the gas. The electrons end up quite a bit hotter than the ions, since the electrons carry the electrical current or absorb the electromagnetic energy, but the presence of the vessel means there is neither time nor space for thermal equilibrium.

4. Origins of species in plasmas

A laboratory gas discharge is confined; that is it has physical boundaries—see figure 4. Charged particles are created and lost both within the volume and at the confining surfaces to varying degrees. Not only does this provide a finer classification of plasmas but also it hints at the possible scaling issues for plasma sources.

Table 1 lists various reactions that can take place at a surface exposed to a plasma. The first two concern etching and deposition processes that are in turn enhanced by the arrival of energy brought by other particles. Tables 2 and 3 list phenomena that take place in the gas phase, where particles are ionized, some molecular gases are broken up and others agglomerate (oligomerize). The last process is the first stage in the formation of particulate matter in plasmas.

4.1. Surface production of electrons

The lowest energy required to remove an electron from a solid is the so-called work function ($e\phi$). Lesser quantities of energy simply will not do the job (quantum mechanics). The energy can arrive in various forms: thermal (phonons, kT), photons ($h\nu$), internal potential energy of atoms and ions (eV_*, eV_i), kinetic energy ($\frac{1}{2}mv^2$, $\frac{1}{2}Mv^2$).

(i) The flux of electrons from thermionic emission shows a strong temperature dependence with a weaker but significant dependence on materials. The theoretical expression (attributed to Richardson and Dushman) is

$$j = AT^2 \exp(-e\phi/kT) \qquad (\mathrm{A\ m^{-2}\ s^{-1}}). \quad (12)$$

Table 1. Surface reactions.

Reactions	Description	Evidence
$AB + C_{solid} \rightarrow A + BC_{vapour}$	etching	material erosion
$AB \rightarrow A + B_{solid}$	deposition	thin film formation
$e^- + A^+ \rightarrow A$	recombination	major loss process
$A^* \rightarrow A$	de-excitation	
$A^* \rightarrow A + e^-$ (from surface)	secondary emission	Auger electrons
A^+(fast) $\rightarrow A + e^-$ (from surface)	secondary emission	Auger electrons

Table 2. Gas phase reactions involving electrons.

Reactions	Description	Evidence
$e^- + A \rightarrow A + e^-$	elastic scattering	thermal electrons
$e^- + A \rightarrow A^+ + e^- + e^-$	ionization	conductivity
$e^- + A \rightarrow A^* + e^-$	excitation	
$e^- + A^* \rightarrow e^- + A + h\nu$	de-excitation	light emission
$e^- + A^* \rightarrow A^+ + e^- + e^-$	two-step ionization	ionization efficiency
$e^- + AB \rightarrow A + B + e^-$	fragmentation	residual gas analysis
$A^+ + e^- + B + e^-$	dissociative ionization	
$A^- + B$	dissociative attachment	
$e^- + A^+ + B \rightarrow A + B$	volume recombination	plasma decay and steady-state

Table 3. Gas phase reactions involving ions and neutrals.

Reactions	Description	Evidence
$A^+ + B \rightarrow B^+ + A$ 'resonant' for B = A	charge exchange	ion energy spectra
$A^+ + B \rightarrow B + A^+$	elastic scattering	ion energy spectra
$A^+ + B \rightarrow A^+ + B^* + e^-$	excitation	ionization efficiency
$A^+ + B \rightarrow A^+ + B^+ + e^-$	ionization	ionization efficiency
$A + B^* \rightarrow A^+ + B + e^-$	Penning ionization	ionization efficiency
$A^+ + BC \rightarrow A^+ + B + C$	fragmentation/dissociation	residual gas analysis
$e^- + A^+ + B \rightarrow A + B$	volume recombination	plasma decay
$A^\pm + B \rightarrow AB^\pm$	oligomerization	ion mass spectra
$A + B \rightarrow AB$	oligomerization	residual gas analysis

Table 4 gives some data on thermionic emission for various materials. The work function is sensitive to crystal orientation and purity. Richardson's theory predicts a value for the constant A that is larger than generally observed.

Photons are effective removers of electrons provided that

$$h\nu > e\phi$$

the excess energy being in the kinetic energy of emitted electrons. Data in table 4 indicate that ultraviolet (UV) radiation will give rise to photoemission whereas visible radiation (<3 eV) will not (λ (in μm)$= 1.2/E$ (in eV)). Very energetic photons (e.g. x-rays) release inner shell electrons from the atoms and the spectrum of emitted electrons gives a signature characteristic of the material (cf the analytical technique 'XPS').

(ii) An important source of energy for electron emission from surfaces at plasma boundaries is in the internal energy of particles such as ions and excited states (especially the metastable ones). In the case of positive ions, recombination on a surface releases to that surface an amount of energy equivalent to that invested in the ion's production, namely eV_i, the ionization energy. If the total ion energy exceeds twice the work function of the surface $\frac{1}{2}Mv^2 + eV_i \geqslant 2e\phi$ then in addition to neutralization a secondary electron *may* be released. Escape from the material is still subject to a statistical factor. Table 5 shows ionization energy data for a range of gases; comparison with work function data in table 4 shows that the threshold condition above is usually met even without taking account of the kinetic energy of incident ions. Neutralization of 10 or 100 eV ions in practice seems to release secondary electrons with almost equal effectiveness. Typical values are given in table 6, in which γ_i records the effectiveness of electron release being the average number of electrons per incident ion. High energy electron impact (100s of eV) is also effective in releasing electrons.

(iii) Electric fields of around 10^8 V m^{-1} are enough to pull electrons directly out of solids in measurable quantities. This kind of field is most easily achieved around sharp features.

4.2. Surface production of positive ions

Bombardment by a stream of high-energy particles can lead to the formation of positive ions on or near surfaces in quantities useful for analytical purposes (cf SIMS). Hot surfaces (2000 K) of high work function materials will ionize low ionization energy atoms, some ions of the hot surface material would also be produced. At lower temperatures (1200 K) metal ions can be derived thermionically from salts coated on filaments. None of these mechanisms is

Table 4. Thermionic emission data. The theoretical value of A is 1.2×10^6.

Material	ϕ (eV)	A (A m^{-2} K^{-2})	Electrons (m^{-2} s^{-1}) at 2000 K
W	4.5	6.0×10^5	8.2×10^{19}
BaO	3.4	2.5×10^4	1.7×10^{21}
ThO_2	2.9	1.6×10^2	2.0×10^{20}
Al_2O_3	3.8	1.4×10^4	9.5×10^{19}
Cu	4.4	6.5×10^5	1.4×10^{20}
Si	4.9	—	—

Table 5. Excitation (V^*) and ionization (V_i) energies of various atoms and molecules.

Gas	V_* (eV)	V_I (eV)	Ionization process
H_2	7.0	15.37	$H_2 \rightarrow H_2^+ + e^-$
		18	$H_2 \rightarrow H^+ + H + e^-$
		26	$\rightarrow H^+ + H$ + kinetic energy + e^-
		46	$\rightarrow H^+ + H^+$ + kinetic energy + e^-
H		13.6	$H \rightarrow H^+$
N_2	6.3	15.57	$N_2 \rightarrow N_2^+ + e^-$
		24.5	$\rightarrow N^+ + N + e^-$
O_2	7.9	12.5	$O_2 \rightarrow O_2^+ + e^-$
		20	$\rightarrow O^+ + O + e^-$
Ar	11.7	15.7	$Ar \rightarrow Ar^+ + e^-$
He	21.2	24.5	$He \rightarrow He^+ + e^-$
CO	6.2	14.1	$CO \rightarrow CO^+ + e^-$
		22	$\rightarrow C^+ + O + e^-$
		24	$\rightarrow C + O^+ + e^-$
		44	$\rightarrow CO^+ + e^-$
CO_2	3.0	14	$CO_2 \rightarrow CO_2^+ + e^-$
		19.6	$\rightarrow CO + O^+ + e^-$
		20.4	$\rightarrow CO^+ + O + e^-$
		28.3	$\rightarrow C^+ + O + O + e^-$
NO	5.4	9.5	$NO \rightarrow NO^+ + e^-$
		21	$\rightarrow O^+ + N + e^-$
		22	$\rightarrow O + N^+ + e^-$
NO_2	—	11	$NO_2 \rightarrow NO_2^+ + e^-$
		17.7	$\rightarrow NO + O^+ + e^-$
N_2O	—	12.9	$N_2O \rightarrow N_2O^+ + e^-$
		16.3	$\rightarrow N_2 + O^+ + e^-$
		15.3	$\rightarrow NO^+ + N + e^-$
		21.4	$\rightarrow NO + N^+ + e^-$
H_2O	7.6	12.59	$H_2O \rightarrow H_2O^+ + e^-$
		17.3	$\rightarrow HO^+ + H + e^-$
		19.2	$\rightarrow HO - H^+ + e^-$
HCl	—	13.8	$HCl \rightarrow HCl^+$

Table 6. Secondary electron emission coefficient (γ_i) for impact of slow positive ions (<keV)—indicative values only.

Surface	Ion	γ_i
Al	Ar^+	0.12
Cu	Ar^+	0.06
Si	Ar^+	0.02
Si	He^+	0.17
W	Ar^+	0.10
W	He^+	0.26

particularly useful for filling a large vessel with ions at the concentrations encountered in low and medium pressure gas discharges around 10^{15}–10^{17} m^{-3} (cf figure 3)—that requires volume processes.

4.3. Volume ionization (simultaneous electron and ion production)

Table 5 lists the energies necessary to remove an electron from a range of gas atoms.

(i) Hot gas will ionize itself (effectively through kinetic energy of the random motion of particles). Since 1 eV is equivalent to a kinetic temperature of 11 000 K, one would not expect much thermal ionization below a few thousand kelvin. This is the regime of high-pressure arcs and thermal equilibrium,

$$A + B^{(\pm)} \rightarrow A^+ + B^{(\pm)} + e^-.$$

(ii) Matter absorbs photons when their energy exactly matches a transition of electrons between energy levels. That means that photo-excitation of gas atoms is a resonant process (being associated with a transition from one atomic level to another). Transitions between the lower excitation levels are generally in the UV (see table 4) but some of the transitions among the higher lying levels correspond with the visible. Since ionization energies tend to be two or three times the values of work functions, photo-ionization is always associated with deep UV radiation, except when it involves interactions between photons and neutrals already excited to (temporary) higher states.

$$A + h\nu \rightarrow A^+ + e^-$$

$$A^* + h\nu \rightarrow A^+ + e^-.$$

(iii) Long-lived excited states (metastables) can be important sources of ionization among species where the ionization energy of species A is less than the excitation energy of species B

$$A + B^* \rightarrow A^+ + B + e^-.$$

This is known as the Penning effect.

(iv) The major volume ionization process arises from high-energy impacts between electrons and atoms. So, an electron with kinetic energy greater than eV_i for a particular species *can* ionize that species,

$$e^-_{fast} + A \rightarrow A^+ + e^-_{slow} + e^-_{slow}.$$

The ionization event is a statistical process that is summarized in terms of how far an electron travels on average before it takes part in an ionizing collision (for electrons below the ionization energy this is essentially an infinite distance). This is called the mean free path for ionization, λ_i.

The way to describe the probability of an ionizing collision is as for elastic processes. Suppose the number density of gaseous atoms is n_g and that an electron travels, as shown in figure 5, into a volume measuring xy in cross sectional area by z in depth. The number of target atoms of gas in the volume is $n_g xyz$.

Suppose each target appears to have a cross sectional area σ_i obstructing the electron path. But now, more realistically, σ_i is some effective cross section that depends strongly on the energy of the electron encountering the gas

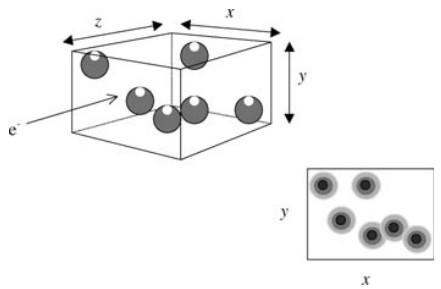

Figure 5. Calculation of ionization cross section—in the xy section the dependence of the cross section on electron energy is represented schematically.

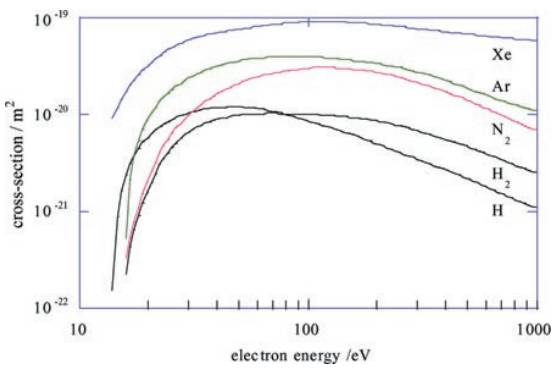

Figure 6. Ionization cross sections for various gases.

(strictly the total kinetic energy in the encounter). The quantity σ_i conveniently describes the probability of ionizing collisions, being zero below the threshold energy (cf figure 2, figure 6 and table 5). For one particular energy of the electron, the whole of the section x–y will be obscured (on average) by the cross section of at least one atom, when $z = \lambda_i(\varepsilon)$ and $(n_g xy\lambda_i(\varepsilon))\sigma_i(\varepsilon) = xy$ or $\sigma_i(\varepsilon) = 1/n_g\lambda_i(\varepsilon)$. When there is a distribution of electron energies the way to find out the effective ionization rate is in principle straightforward. One adds together the contributions of the various energy subgroups, into which the population can be divided, weighting each according to the population of the group to make a kind of average ionization frequency. It is written mathematically as follows

$$\nu_i = \frac{n_g \int_0^\infty \sigma_i(v) v f(v)\,\mathrm{d}v}{\int_0^\infty f(v)\,\mathrm{d}v} \qquad (13)$$

in which $f(v)$ is the energy distribution function of the electrons and $f(v)\,\mathrm{d}v$ does the weighting. The integration in the numerator does the adding and the denominator completes the weighted averaging.

Figure 7 shows the same thing pictorially. This kind of analysis leads to the conclusion that the rate of volume ionization by a Maxwellian group of electrons is a very strong function of temperature, since it is very sensitive to the population in the tail of the distribution. Figure 8 shows the volume excitation and ionization rates for argon, by a Maxwellian group of electrons, as a function of electron temperature.

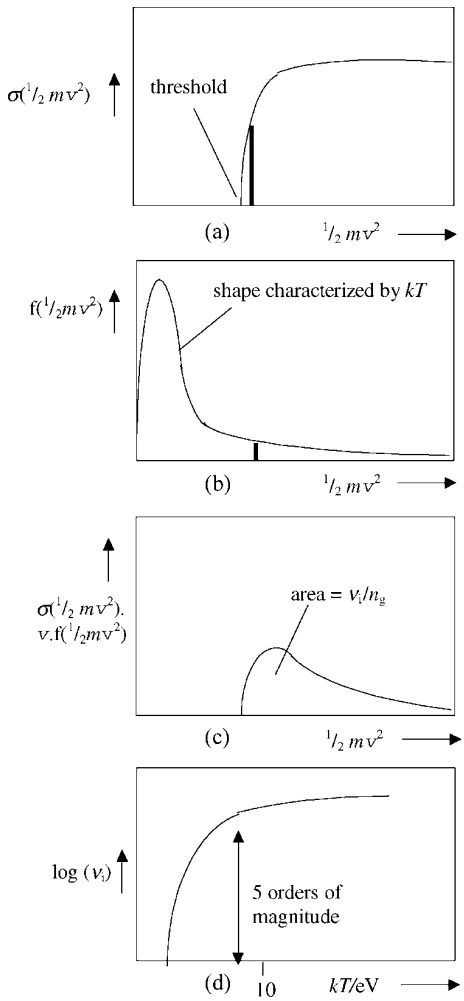

Figure 7. Calculation of collision frequency: (a) cross-section; (b) EEDF; (c) integrand for collision frequency calculation; (d) collision frequency (log scale) against kT.

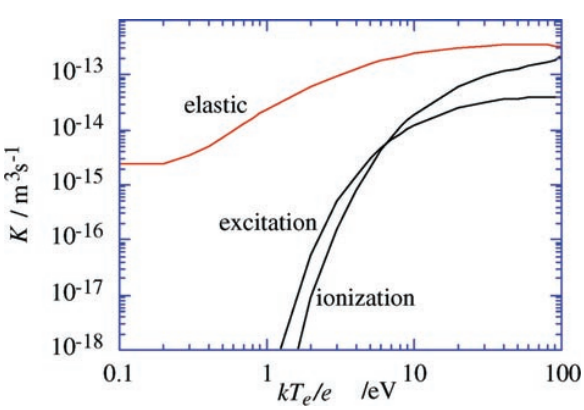

Figure 8. Rates for argon.

4.4. Electron attachment (negative ion formation)

When an electron collides with a neutral gas atom or molecule it may become attached, forming a negative ion. This process depends on the energy of the electron and the nature of the gas. For example, O^-, O_2^-, NO_2^-, NO_3^-, OH^-, H^- and the negative halogen ions are readily formed but not N^-, N_2^- or

negative ions of the rare gases. In the attachment

$$A + e^- \rightarrow A^- + h\nu$$

$$AB^* + e^- \rightarrow A^- + B$$

the energy liberated is any internal energy plus kinetic energy plus the binding energy, E_a (about 1.5 eV for O, 4 eV for F, Cl and 0.7 for H; the molecules of oxygen and the halogens have binding energies around 0.5 eV).

The mechanisms of attachment involve the formation of intermediate states. In general, cross sections are around 10^{-24} m^2. Dissociative attachments have thresholds of a few eV.

Negative ions can be destroyed, e.g. by collision with atoms, electrons, or photons. The reaction $O^- + h\nu \rightarrow O + e^-$ starts when $h\nu \geqslant 1.5$ eV and $\sigma \approx 1 \times 10^{-21}$ m^2 at $h\nu \geqslant 2.75$ eV. Detachment of an electron from H^- by light starts at $h\nu \approx 0.7$ eV; it rises to 4.5×10^{-21} m^2 at $h\nu = 1.5$ eV and decreases at higher energies.

4.5. Volume recombination

Simple electron–ion recombination is not a straightforward process. The photo-ionization route involves very little momentum so the reverse process requires virtually stationary electrons and ions. The electron impact ionization route produces three particles so reversing it needs three bodies to come together to conserve energy and momentum:

$$e^- + e^- + A^+ \rightarrow A + e^-_{faster}.$$

One way in which volume recombination is facilitated is through attachment followed by an ion–ion recombination in a second step

$$e^- + AB \rightarrow AB^-$$

$$AB^- + C^+ \rightarrow AB + C$$

4.6. Surface recombination

The constraints of energy and momentum conservation are easier to satisfy for recombination in interactions of three or more bodies. The physical boundaries of laboratory discharges are an effective third body. Recombination on the walls is the major loss process for discharges at low pressure, almost by definition. The energy released by recombination then passes into the wall; see section 4.1.

5. Breakdown

In this section the process of electrical breakdown is considered. If an electric field is applied to a plain parallel gap of width d, containing a gas, at sufficiently high fields the gas suddenly switches from being insulating dielectric to conducting gas. It is supposed that a few electrons are always around in the gap, either by the action of cosmic rays or else as a consequence of field emission from asperities on the surface, close to which electric fields are strongly enhanced.

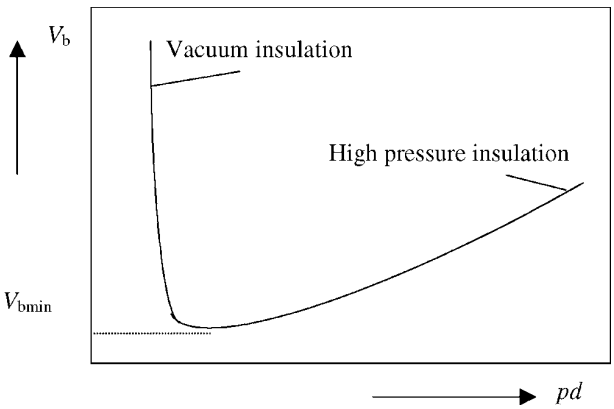

Figure 9. Schematic breakdown curve for a parallel plate.

5.1. Drift

The motion of charged particles is a combination of random thermal activity and the steady drift superimposed by electric fields. Often it is useful to concentrate on the steady drift component alone. For instance in the initial breakdown phase of a gas discharge one is interested in a few electrons interacting in isolation with a background gas. The balance of forces involves the effect of the electric field $(-eE)$ on the electrons and the rate of change of particle momentum $(mv\nu)$, where it is supposed that electron momentum is transferred to the gas in collisions that take place with a frequency ν. It follows that for this model the mean free path between collisions must be much smaller than the size of any containing region, $\lambda \ll d$; (in Ar: $\lambda \sim 1/3$ mm at 1 Torr). The drift speed is then related to the electric field by the mobility, μ:

$$v_{drift} = \left(\frac{e}{m\nu}\right) E = \mu E. \tag{14}$$

In general the mobility decreases as pressure increases. Strictly it is a function of electron energy but simple models treat it as constant. Kinetic theory links diffusion to mobility through the Einstein relation $D/\mu = kT/e$.

5.2. Multiplication

After one mean free path for ionization (λ_i), an electron produces on average one electron ion pair. So the increase in the number of electrons that can be expected in any slab of gas of thickness dx between the plates is

$$dN = N\,dx/\lambda_i \tag{15}$$

where N is the local number of electrons. As a result, the electron (and positive ion) population grows ('multiplies') exponentially with distance:

$$N = N_0 \exp(x/\lambda_i). \tag{16}$$

5.3. Townsend's coefficient (α)

Townsend related the ionization mean free path to the total scattering mean free path (λ) by treating it as being a process activated by drift energy gained from the field ($E\lambda$), with an

activation energy eV_i. This leads to a formula analogous to that of Arrhenius for thermally activated processes, giving rate constant known as Townsend's ionization coefficient

$$\alpha = \frac{1}{\lambda_i} = \frac{\text{constant}}{\lambda} \exp\left(\frac{-V_i}{E\lambda}\right).$$

Since the mean free path is inversely proportional to pressure (p), the coefficient can be written

$$\alpha = Ap \exp\left(\frac{-Bp}{E}\right) \tag{17}$$

where the constants A and B are properties of the gas.

5.4. Self-sustained by secondary emission

Next, attention is turned to the consequences of the subsequent motion of the positive ions. Acceleration of the positive ions in the electric field leads, in principle, to secondary emission of electrons from the negative electrode, when they reach there, at a rate of γ electrons per incident ion; see section 4.1. The processes of secondary emission and multiplication will become self sustaining if the ions from multiplication between $x = 0$ and $x = d$ release from the cathode sufficient secondaries to exactly replenish population of ions in the gap. According to equations (15) and (16) N_0 initial electrons will produce $\alpha N_0 \exp(\alpha x)\,\mathrm{d}x$ ions in the slab $\mathrm{d}x$ at position x. Across the gap therefore there will be generated $N_0[\exp(\alpha d) - 1]$ ions. To be self-sustaining

$$\gamma N_0[\exp(\alpha d) - 1] = N_0$$

or

$$\alpha d = \ln\left(1 + \frac{1}{\gamma}\right). \tag{18}$$

5.5. Paschen's law

Combining (16) and (17),

$$Apd \exp\frac{-Bp}{E} = \ln\left(1 + \frac{1}{\gamma}\right).$$

In planar geometry, $V_b = Ed$, so

$$V_b = \frac{Bpd}{\ln(Apd) - \ln[\ln(1 + \gamma^{-1})]}. \tag{19}$$

At large pd, V_b increases—high-pressure insulation. At some critical value of pd, V_b goes infinite—vacuum insulation. In between, there is a minimum; see figure 9.

5.6. RF breakdown

The above assumes dc conditions. RF breakdown is similar except that at a high-frequency surface processes are not so important: electrons are confined by field oscillations—multiplication replenishes diffusive losses. As with dc (and low-frequency) breakdown, higher values of pd require larger voltages to achieve breakdown and at low pd there is again a sharp rise in breakdown voltage.

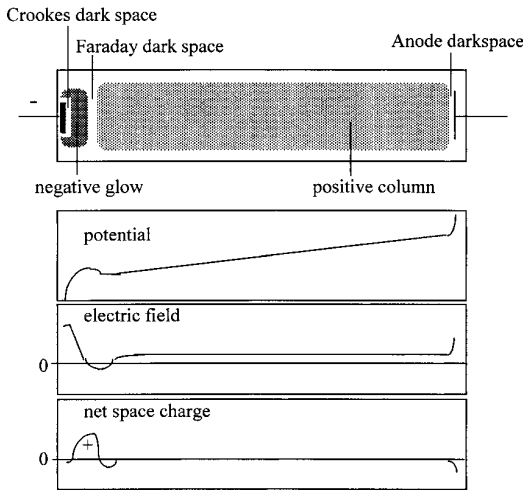

Figure 10. Schematic structure of a dc discharge.

6. Discharge structure

The classical laboratory discharge is modelled on a tubular (long-cylinder) discharge lamp. In this section the axial and 'radial' structure is examined; for simplicity here rectangular rather than cylindrical geometry is treated. Steady current (or low-frequency alternating current (ac)) flows in the axial direction. At right angles to the current flow the discharge is confined but there is no net current to the boundaries. Discharges in other geometries show equivalent features to those described below.

6.1. The axial structure

Figure 10 shows the conventional axial picture. The intensity of shading implies visible brightness. Fluorescent lamps largely sacrifice this light in favour of emission from the coating of fluorescent material on the glass wall of the tube stimulated by the ultra violet emission from the plasma; see section 4. In the figure the following regions are identified.

- Negative glow—here intense ionization (and excitation) produces species that maintain secondary processes at the cathode. This region is necessary if the discharge is self-sustaining; see section 5.4.
- Positive column—this region extends the conducting medium (plasma) along most of the remaining length of the tube at the price of E (V m^{-1}); in a uniform tube E is constant, so that the voltage across the positive column increases in proportion to its length.
- Faraday dark space—this zone matches negative glow to positive column.
- Crookes, anode and radial boundary 'dark spaces'—space charge sheath regions; see section 6.2.

Discharges conduct current owing to the mobility of the component charges; electrons are the dominant carrier, unless they are strongly impeded by, for instance, attachment (see section 4.4) or magnetic fields.

Along the direction of current flow the electrons move with a drift plus a random velocity. The drift component (v_d) is proportional to the electric field (E)

$$v_d = \mu E$$

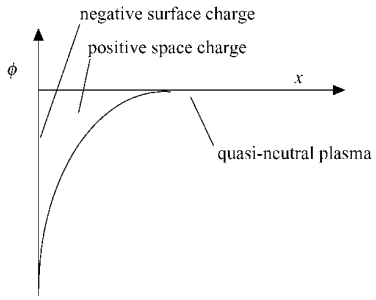

Figure 11. Potential structure in a sheath.

and the current density is given locally by

$$j = nev_d = ne\mu E.$$

The structure of higher frequency discharges differs somewhat. Near the electrodes displacement current lessens the requirement for the physical action of the negative glow in maintaining the continuity of current at the negative electrode.

6.2. Plasma boundaries—space charge sheaths

Electron impact ionization provides a continuous source of charged particles in the volume of a discharge plasma. At low pressure (i.e. when volume recombination is relatively unimportant), gradients must therefore become established to drive an equivalent loss. Gradients in potential give rise to electric fields that accelerate the heavier, less mobile, positive ions while simultaneously slowing electron loss.

The potential structure is initiated by negative charge that is quickly established on surfaces exposed to the plasma through the arrival of the more energetic electrons. Adjacent to the surface charge is a boundary layer of positive space charge, extending over a narrow region of space across which the potential changes rapidly; see figure 11. Poisson's equation relates potential structure to space charge, ρ:

$$\frac{\mathrm{d}^2\phi}{\mathrm{d}x^2} = -\frac{\rho}{\varepsilon_0}. \tag{20}$$

The scale length, l, of the sheath region can be estimated by the dimensional argument

$$\frac{\phi}{l^2} \approx -\frac{n_i e}{\varepsilon_0}.$$

With $\phi \sim kT_e/e$ and $n_i \sim n_0$, the plasma density,

$$|l| \approx \sqrt{\frac{\varepsilon_0 kT_e}{n_i e^2}} \tag{21}$$

which is known as the Debye length; it is the scale length of space charge regions where potentials comparable with or larger than kT_e/e occur.

In the plasma, potential changes much more slowly on a scale length of L, which is effectively the size of the containing vessel.

$$\frac{\mathrm{d}^2\phi}{\mathrm{d}x^2} = \frac{(n_e - n_i)e}{\varepsilon_0}$$

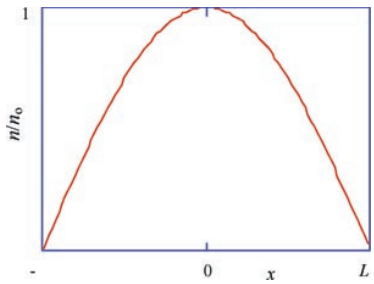

Figure 12. The cross sectional profile.

so

$$\frac{\phi}{L^2} \approx \frac{(n_e - n_i)e}{\varepsilon_0}.$$

Since in the plasma $n_e \sim n_i$ the potential changes only over relatively large distances.

As electrons and ions leave the quasi-neutral plasma, passing into the boundary sheath, a positive space charge must develop and the potential must fall, according to the argument above. So, entering from the plasma

$$\frac{\partial\rho}{\partial V} = \frac{\text{+ve change in space charge}}{\text{−ve change in potential}} < 0.$$

This condition sets a criterion for the speed at which ions enter the sheath. Assume the electrons are in thermal equilibrium with the local potential and so the Boltzmann factor can be applied; strictly this requires there to be virtually no net electron flux, compared with the random thermal flux

$$n_e = n_s \exp(e\phi/kT_e)$$

where n_s is plasma density at the sheath–plasma boundary and in the sheath $\phi < 0$. The sheath is relatively thin and so ions can reasonably be expected to pass into it without collisions. It is assumed therefore that ions are in free fall from the sheath–plasma boundary where their kinetic energy is $\frac{1}{2}Mc_s^2$ and their flux is $n_s c_s$. It follows that the ion flux is conserved and that at any point within the sheath the ion density is given by

$$n_i = \frac{n_s c_s}{\sqrt{c_s^2 - 2e\phi/M}}.$$

Applying the above criterion on the space charge variation gives

$$c_s^2 \geqslant \frac{kT_e}{M}. \tag{22}$$

This is called the Bohm criterion; usually, the equality is sufficient. It shows that positive ions must be expelled from the plasma into the space-charge boundary with a minimum speed. It therefore quantifies the ion particle flux ($n_s c_s$) at a normal plasma boundary.

6.3. Steady state discharges (zero-dimensional model) I: density

The energy supplied to a discharge ends up in heat, light and chemistry; see section 7. To a large extent it can be accounted

for as heat, arriving at surfaces with the particle fluxes leaving the plasma

$$P_{in} = n_s c_s(T_e) A_{eff} [\varepsilon_c(T_e) + \varepsilon_s(T_e) + 2T_e].$$

The energy contributions to the right-hand side are as follows. The first accounts for the average cost per electron for producing one electron–ion pair (ionization energy plus an extra amount to account for losses in non-ionizing collisions—the extra being less as T_e increases). The second relates to energy taken specifically by ions, accelerated in space charge boundary layers, and delivered to surfaces as ions (and or fast neutrals). Axially this may be comparable with the discharge voltage; radially it is dependent on the boundary physics. The third term accounts for the drain on the electron thermal energy.

So, rearranging,

$$n_s = \frac{P_{in}}{c_s(T_e) A_{eff} [\varepsilon_c(T_e) + \varepsilon_s(T_e) + 2T_e]}. \tag{23}$$

This relationship suggests that the density of a discharge plasma can be expected to increase with input power and that the power can be used more effectively to obtain a denser plasma if the electron temperature is higher (ionization is more efficient so the term $\varepsilon_c(T_e)$ is smaller) and, or, the potential across boundary sheaths is lower (the term $\varepsilon_s(T_e)$ is smaller).

6.4. Steady state discharges (zero-dimensional model) II: temperature (assumed Maxwellian)

At low to medium pressure, in simple discharge media, volume production balances surface loss. The particle balance therefore requires that

$$K_{iz}(T_e) n_g n_e V_{eff} = n_s c_s(T_e) A_{eff}$$

where $K_{iz} n_g$ is effectively the ionization rate, ν_i discussed in section 4 and $n_s c_s(T_e)$ is the particle flux at the boundaries. The term $c_s(T_e)$, is not strongly dependent on T_e. So

$$\frac{K_{iz}(T_e)}{c_s(T_e)} = \frac{1}{n_g L} \tag{24}$$

where geometric terms (including n_e/n_s, which is the ratio of average electron density to that at the boundary) are combined to give L, the effective characteristic size of the system. This expression effectively sets T_e for any given pressure (n_g) and geometry (L).

The rate constant for ionization, K_{iz}, is generally a strong function of T_e covering five orders of magnitude for argon over the range 1–10 eV; see figure 8.

6.5. Steady state discharges (zero-dimensional model) III: electric field

In a steady state dc discharge the electrons gain energy by moving through the electric field in the bulk of the plasma. Energy is lost locally at the same rate to the background gas, predominantly by elastic collisions. So,

$$eE v_d = \frac{e^2 E^2}{m\nu} = \delta \frac{3}{2} k(T_e - T_g)$$

where δ is the fraction of energy transferred in an elastic collision (maximum $2m/M$ for electron gas collisions) and ν is the frequency of collisions. This suggests that

$$\frac{(T_e - T_g)}{T_e} \approx \frac{M}{m} \frac{eE}{kT_e} \lambda. \tag{25}$$

So at low pressure, when mean free paths are relatively long, the electrons remain much hotter than the gas; conversely, at high pressures, thermal equilibrium can be approached.

A crude estimate of the electric field in a self-sustaining plasma can be obtained by supposing that electrons travel their entire free path in the direction of the field and lose all the energy gained in an optimum collision with the (cold) gas

$$E\lambda \approx \frac{m}{M} \frac{kT_e}{e}$$

(which suggests a scaling of temperature with E/p, though this is not always the case in practice). This gives several volts per centimetre at 1 Torr in argon. A better model would take proper account of the collision dynamics.

More complex scenarios occur in molecular gases and elsewhere when inelastic collisions play a significant part in the local energy balance.

6.6. Discharge structure II (Schottky—medium pressure, 1-dimensional)

Here the basic structure perpendicular to the direction of current flow is quantified in a regime where electric fields and diffusion jointly determine the particle fluxes. The scenario is this. To ensure that volume-production equals wall-loss an electric field must develop to drive ions out while slowing the loss of electrons, that would otherwise be excessive. This electric field acts in conjunction with the diffusion of particles down gradients of density. One dimensional equations for the ion and electron fluxes arising from the combined effects of diffusion and electric field driven drift are:

$$\Gamma_i = -D_i \frac{\partial n_i}{\partial x} + n_i \mu_i E \tag{26}$$

$$\Gamma_e = -D_e \frac{\partial n_e}{\partial x} - n_e \mu_e E \tag{27}$$

where D_i, D_e are diffusion coefficients, for which values can be estimated.

6.6.1. Ambipolar diffusion. In the plasma the charged particle densities are the same. The drag between energetic thermal electrons and the positive ions gives rise to an effective diffusive loss of particles with positive and negative charges both leaving the volume at the same rate (ambipolar diffusion). The net diffusive flux is associated with a gradient in the species density ($n_e = n_i = n$) and a hybrid diffusion coefficient that can be obtained by equating the fluxes and eliminating the electric field from equations (27) and (28)

$$\Gamma = -D_a \frac{\partial n}{\partial x}$$

where D_a is the ambipolar diffusion coefficient.

6.6.2. Ionization. Electrons and ions are created at equal rates primarily by electron impact

$$\frac{\partial n}{\partial t} = \nu_i n.$$

6.6.3. Steady state. The divergence of the flux balances the source (and sink) terms, giving in planar geometry

$$-\frac{\partial}{\partial x} D_a \frac{\partial n}{\partial x} = \nu_i n.$$

Taking the ambipolar diffusion coefficient to be constant, the solution is

$$n = n_0 \cos(\pi x / L)$$

where $(\pi/L)^2 = \nu_i / D_a$. Fitting the profile to the vessel (L) selects the ionization rate (ν_i) and hence the electron temperature; this is similar to the result in section 6.4 that was used to estimate the electron temperature. The model neglects the sheath and implies $n = 0$ at the boundary.

In cylindrical geometry a Bessel function describes the profile.

6.7. Discharge structure III (Tonks–Langmuir—low pressure, 1-dimensional)

A low-pressure model due to Tonks and Langmuir treats ions as falling freely from the place where they have been created, instead of the diffusion mechanism of the previous section. This then gives the ion flux at any point as the sum of all sources upstream. With a free fall ion velocity and the Boltzmann model for electrons, plasma region is mapped out; the boundary is identified with the point where the quasi-neutral assumption fails.

The analysis is complicated and is not included here. The result shows a quasi-neutral plasma with a potential profile which drops smoothly by about 0.85 kT_e before the electric field becomes infinite and the model anticipates the formation of a space charge sheath. In the sheath, the scale length is that of the boundary layer and the potential changes rapidly (see plasma boundaries). A similar infinite field boundary can be obtained by including a momentum transfer term in a simpler mono-energetic ion model. The result is that the quasi-neutral plasma extends over a potential of about 0.5 kT_e where again the electric field becomes infinite.

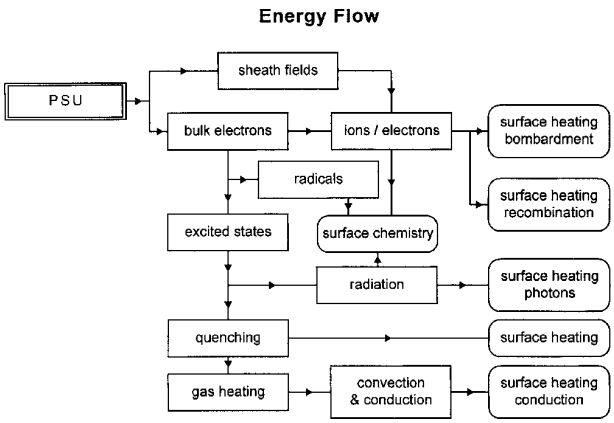

Figure 13. Energy flow in discharge plasmas.

7. Energy flow through a plasma

Finally in this introductory article on gas discharges, the paths by which the electrical energy flows through a laboratory discharge are illustrated. Figure 13 summarizes them for a generic processing plasma. Ultimately, virtually all energy ends up as heat with a small fraction invested in surface chemistry.

8. Conclusion

The purpose of simple discharge models is to reveal the dependencies and scalings to be expected. The ideas described above are all to some extent corroborated by experiments, though care must be taken to check all the assumptions involved, which define ranges of validity. Equally powerful are the fluid and particles simulations which can also be tested against the simpler zero and one-dimensional analytical models.

References

Von Engel A H 1964 *Ionised Gases* (Oxford: Oxford University Press)

Franklin R N 1977 *Plasma Phenomena in Gas Discharges* (Oxford: Oxford University Press)

Lieberman M A and Lichtenberg A J 1994 *Principles of Plasma Discharges for Materials Processing* (New York: Wiley Interscience)

Raizer Y P 1991 *Gas Discharge Physics* (New York: Springer)